

Prevention of the Antimony Compounds at The Geothermal Power Plants with Hydrodis® Ge Products

Ayhan Erten^{1*}, Mustafa Eroglu¹, İrfan Avcı¹, Taylan Karan¹, A. Efekan Çoban¹

Abstract: The energy demand is increasing day by day. Therefore, the renewable and sustainable energy of geothermal power plants is very important. The biggest problems seen in geothermal power plants are sedimentation and scaling. The scaling occurs into the wells, pipelines and heat exchangers, etc. where the geothermal brine passes. Those locations where the elements and compounds in the geothermal brine precipitate under specific conditions, forms scales. Those scales caused decreased efficiency of energy production. During the process of energy production, the temperature drops inside heat exchangers and that causes the antimony (Sb) compounds got precipitated and caused scaling. Those scales negatively affect heat transfer and eventually cause less energy to be produced by causing blockage of the vaporizer, preheater, and filters. For this reason, stibnite scaling is a situation that should be taken into serious consideration. Until now, different methods have been developed against stibnite scalings. As of 2020, HYDRODIS® GE has been formulated and developed by the Bozzetto Group, which the aim of stop the precipitation and cuts the operating costs. In this way, the antimony compounds where possibly creates scales got prevented and returned in the geothermal brine to the reservoir via reinjection wells by letting production continue without any energy loss.

Keywords: Stibnite, antimony, geothermal power plants, HYDRODIS® GE.

¹Address: Bozzetto Group., Istanbul/Turkey

*Corresponding author: ayhan.erten@bozzetto.com.tr

Citation: Erten, A., Eroglu, M., Avcı, İ., Karan, T., Çoban, A.E. (2021). Prevention Of The Antimony Compounds At The Geothermal Power Plants With Hydrodis® Ge Products. Bilge International Journal of Science and Technology Research, 5(2): 146-156.

1. INTRODUCTION

Geothermal wells are used to transfer the hot magma energy under the earth's crust to underground water. Some important places with hot water and convection and upstream steam return are California, New Zealand, Italy,

Turkey, Japan, and Iceland. Among these countries, Turkey has an important position. Turkey, as a country with rich geothermal district heating, is used for greenhouse heating and spa centers with the production of both electricity (Baran vd., 2015).



Figure 1. The BMG (Büyük Menderes Graben) and GG (Gediz Graben) Systems in Western Anatolia. Fig (Haklıdır & Şengün, 2020).

This study was completed at the Gediz Graben, a part of the Turkey. Turkey was strongly affected by the Alpine-Himalayan orogenic belt, which emerged at the confluence of the Eurasian and African Plates, resulting in crustal thickening from tectonic compression in Eastern Anatolia (Haklıdır & Şengün, 2020). Alaşehir geothermal field is one of the high-temperature regions in the Gediz graben and is the region where the geothermal power plant in this study is located. Many geothermal areas in Turkey have are low to medium enthalpy fields, which are the most preferred systems for generating electricity in binary power plants (Baran vd., 2015).

Scaling is a major problem in geothermal applications. Blockage and sedimentation problems caused by scaling reduces power plant production and expensive cleaning and operation costs. The decrease in energy yield and increase in operating costs directly affects financial return. Geothermal fluid chemistry in the different types of scaling can be seen in different geothermal fields and sometimes in different wells of the same site.

The general characteristics of the scales originating from the geothermal fluid depend on the geological environment, reservoir type, physicochemical properties, and hydrogeological and hydrochemical properties, to give an example of natural conditions. However, other properties are due to operating conditions, well depth, flow rate, operating pressure, and operating temperature. However, antimony compounds, which are formed due to the cooling of the geothermal brine, are a type of scale that varies according to power plant designs, power plant electricity energy production demands, and earth crust natural conditions.

Antimony, a constituent of hydrothermally formed mineral paragenesis often in the trivalent state as stibnite (Sb_2S_3), or more commonly known as its members, in the form of thioantimonites of lead, copper, silver, mercury, iron, etc. large group of "sulfosalt minerals". Rarely, it occurs as antimony, the natural element or alloys (antimonides), or as the oxysulfate kermesite (Krupp, 1988). Scaling of stibnite and antimony-rich sulfide has been observed in pipelines at geothermal power plants in various geothermal systems, including Italy, El Salvador, and New Zealand (Olsen vd., 2012). Consequently, Turkey has sulfides of antimony into local to some geographic areas like other countries.

The identity of the species controlling antimony transport in natural high-temperature fluids is not well known, studies to date rely on indirect evidence such as stibnite solubility as a function of pH and dissolved sulfur (Sherman vd., 2000).

Antimony is a silvery, white, brittle, crystalline solid that exhibits poor conductivity of electricity and heat. It has an atomic number of 51, an atomic weight of 122, and a density of 6.697 kg/m³ at 26 °C (Anderson, 2012). However, in geothermal brines, Sb(III) is the oxidation state (Brown, 2011). Stibnite is antimony (III) sulfide Sb_2S_3 . Normally pointed (long, needle-like) occurs naturally as a mineral that forms black crystals (Brown, 2011). Usually, Sb precipitates from geothermal brine as Sb_2S_3 . At low T leaving a heat exchanger the deposits

produced are amorphous, red, or orange "Metastibnite"; at high T the black mineral Stibnite is sometimes produced (Weres, 2019). Sb (III) complex in addition to sulfur, which may be important in several metastibnite geological, Sb (V) are sulfur complexes. The thioantimonate complexes SbS_3 , $\text{SbS}(\text{HS})^+$, and $\text{Sb}(\text{HS})_4^+$ have long been known experimentally. Seems to contain few minerals. Sb(V) in fourfold coordination with sulphur: famatinite, Cu_3SbS_4 ; potosiite, $\text{Pb}_6\text{Sn}_2\text{Fe}_2\text{Sb}_2\text{S}_{16}$; and stibioenergite $\text{Cu}_3(\text{Sb,As})_4$ (Sherman vd., 2000). Metastibnite is an amorphous (non-crystalline) colloid and is red-colored (Brown, 2011). However, the stibnite is normally observed in dual plant preheater (Brown, 2011). In binary plants, stibnite, usually red amorphous form is precipitated as black rather than crystalline form (Brown, 2011). The antimony species likely to be present in the geothermal brine have been characterized by Krupp (Krupp, 1988).

His experiments investigated the equilibrium between stibnite and several soluble sulfide complexes (Scanes, 1989). Although there may be antimony concentration is too low in the brine, it may become almost quantitative scaling antimony sulfide (Brown, 2011). Antimony sulfur solubility is very sensitive to temperature and pH changes. Some studies of the dual plant may experience both lower pH at a lower temperature. Specifically, the steam is condensed in an evaporator and then added to the brine and then directed to a preheater where low temperature and low pH are likely (Brown, 2011). Stibnite (Sb_2S_3) is the most abundant mineral antimony and resolution, the primary control over the concentration of antimony hydrothermal fluid (Olsen vd., 2012).

Binary plants often have lower brine temperatures than conventional flash plants. Also, pH modification or addition of brine due to the capacitor should have a low pH. Under these conditions, antimony(III) sulfide (stibnite) may precipitate in the heat exchangers, causing loss of heat transfer and ultimately clogging of the heat exchanger tubes (Brown, 2011). Mechanical cleaning, steam cleaning, and caustic soda washing options are available today to prevent stibnite deposits (Brown, 2011).

Although the plant uses a polyacrylate inhibitor to control calcite deposition, this was found to be ineffective for stibnite deposition (Scanes, 1989). For stibnite, it is possible to develop antiscalants such as calcite antiscalants. Some research has been done in this area, but there is no antiscalant on the market yet that is successful in preventing stibnite deposition. However, research continues (Brown, 2011).

The literature has reported a few negative results of the trial on stibnite. The last development of Bozzetto Group has pretended stibnite scales into the geothermal system.

2. MATERIAL AND METHODS

As of 2020, studied by the Bozzetto Group to evaluate the performance of HYDRODIS® GE to inhibit antimony sulfide deposition in geothermal brines under dynamic

conditions. This study was carried out in the 24 MW power plant in Alaşehir, Manisa.

In this study, the geothermal power plant has one vaporizer and two preheaters. The brine inlet temperature at average 170 °C and HYDRODIS® GE was injected through power plants pipelines designed by Ormat Energy Converter (OEC) units. The average brine outlet temperature was average 65 °C for the preheater outlet. Typical brine flow rates were 825 tonnes/hours.

In this study, we planned to dose the maximum quantity as 15 ppm and optimize it by week. So, the controls were provided by dosing the inhibitor at 15 ppm in the first two weeks. After 15 ppm of the first phase of the test, the coupons and filters were removed, observed physically, and analyzed with XRF, and then the optimization was provided according to the results of the analysis.

By the way, the checked coupons and the filters have been inserted into the system without cleaning and were observed every week during the trial period. During the optimization study, the dosages were reduced from 15 ppm to 10 ppm and 5 ppm. Finally, 5 ppm dosage provided stability and did not change the brine's chemistry.

3. RESULTS AND DISCUSSION

The brine chemistry data, filters, coupons were observed throughout the trial. The following data which obtained during the trial was performed by the XRF analysis made

on the filters together with the physical observation of them.

The XRF analysis of the filter samples was carried out with the X-MET8000 Expert XRF device. The scale deposit was investigated using Scanning Electron Microscopy (SEM), while providing high magnification images, SEM can also provide a semi-quantitative elemental analysis of the scale deposits. SEM analyzes of the samples obtained were carried out with the Fei Quanta 250 Feg and EdX analysis with the EDX Detector (Oxford Aztec) device. The scale deposit was investigated using X-Ray Powder Diffractometry (XRD) while providing information about the chemical composition and crystallographic structure of scale deposits. XRD analyses were carried out on the Philips X'Pert Pro device. The scales on Xrd analyzed at the 2θ theta and 5-80 degrees Cu Kα radiation with a wavelength of 0.1542 nm.

3.1. The effect of HYDRODIS® GE to geothermal brine chemistry

The effect of HYDRODIS® GE products on brine chemistry is given in Figures 2,3,4 and 5. According to brine chemistry analysis, it was observed that the values were stable without any change in the silica and total hardness data. Obtaining parallel values at the inlet and outlet of the plant shows that our product named HYDRODIS® GE provides high stability even in optimization studies with low dosage products without being affected by dosage changes.

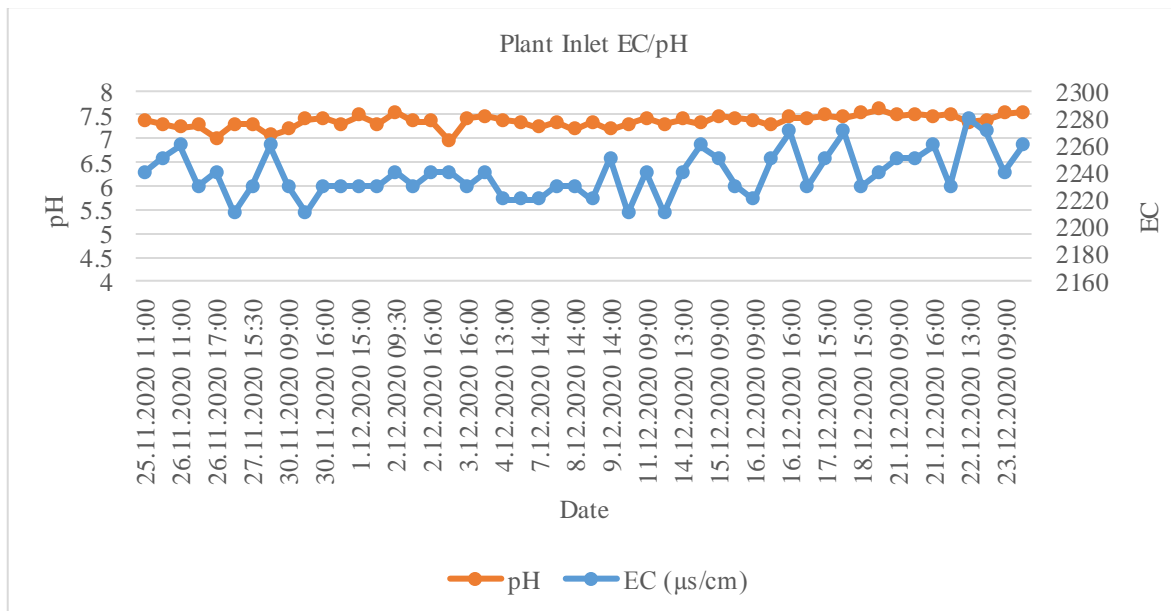


Figure 2. The effect of HYDRODIS® GE on ec/ph of plant inlet of brine chemistry

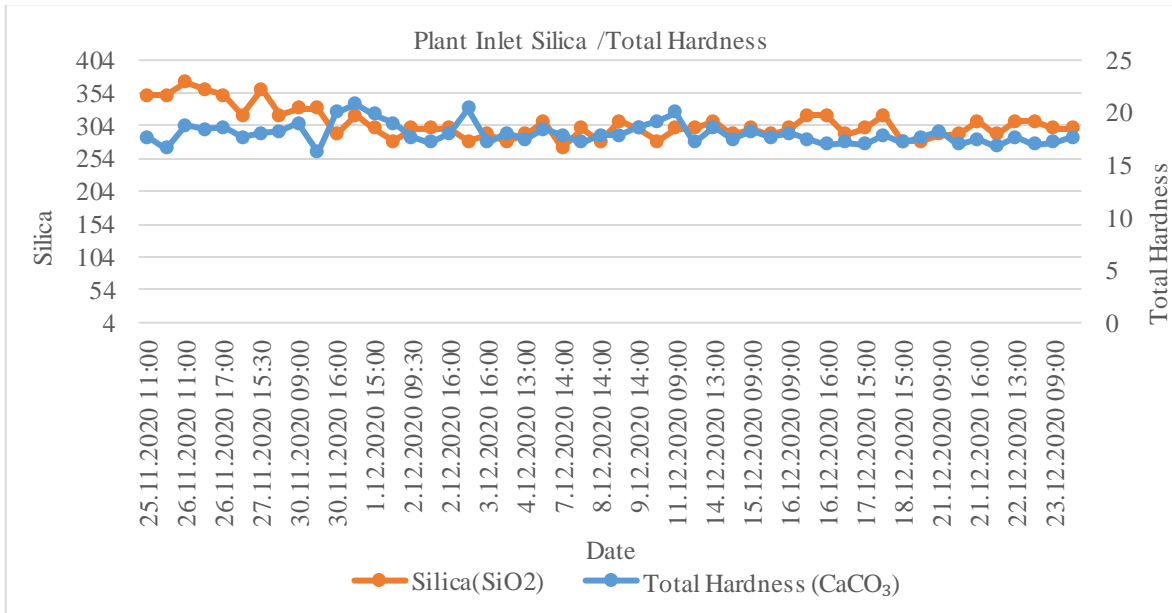


Figure 3. The effect of HYDRODIS® GE on silica and total hardness of plant inlet of brine chemistry

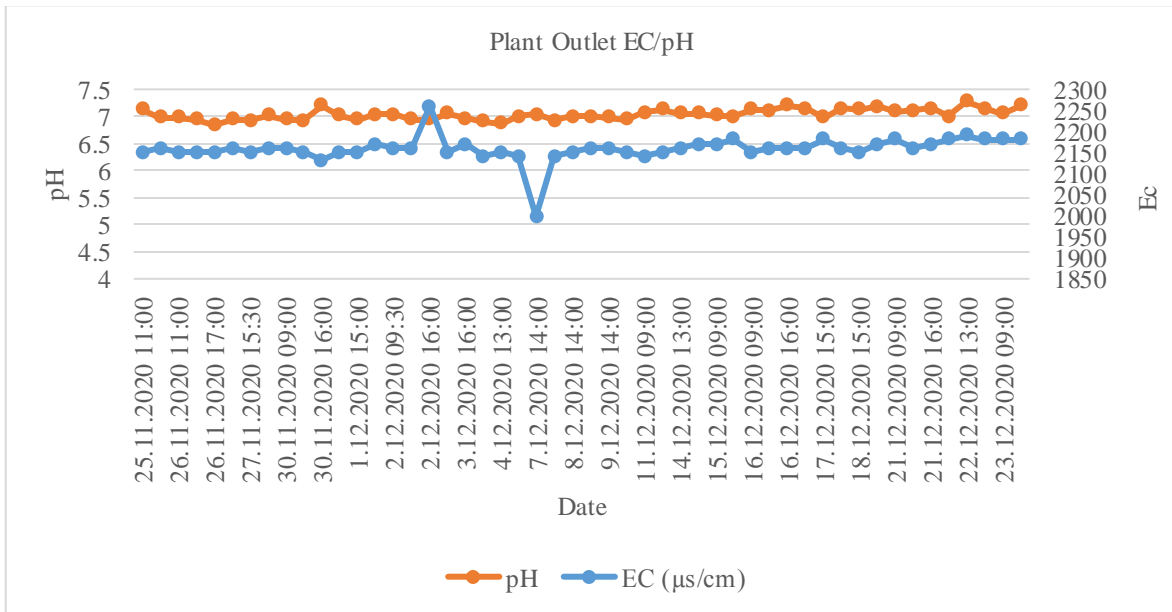


Figure 4. The effect of HYDRODIS® GE on EC/pH of plant outlet of brine chemistry

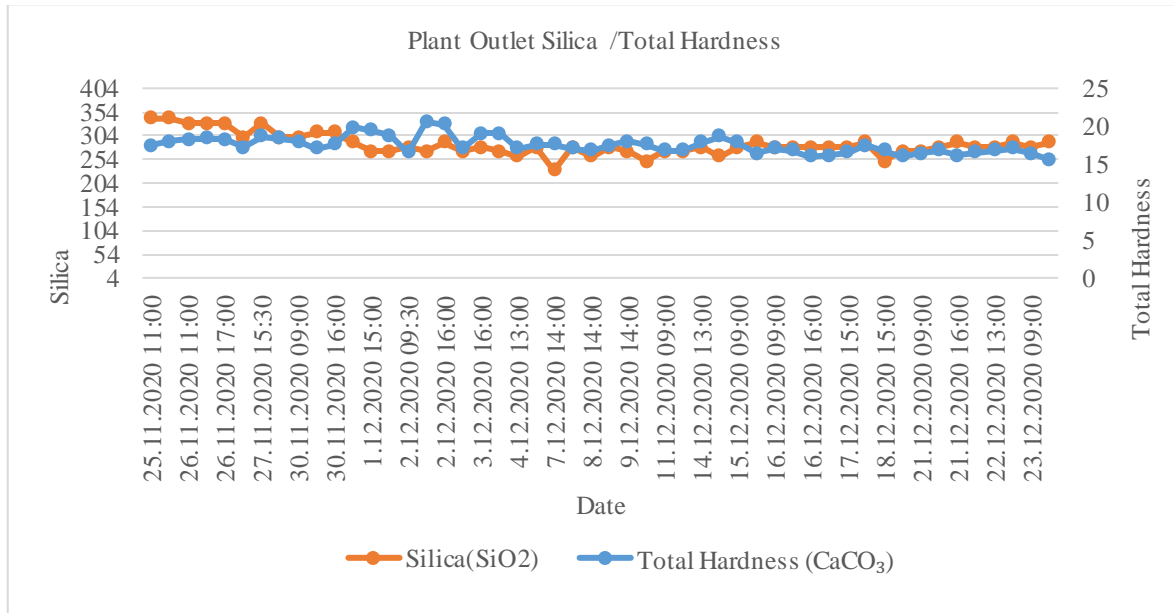


Figure 5. The effect of HYDRODIS® GE on silica and total hardness of plant outlet of brine chemistry

3.2. The effect of HYDRODIS® GE to scales of filter

The effect of HYDRODIS® GE products on scales of filters are given in Table 1 and Figure 6. Antimony (dark brick color) precipitation seen in the injection filter (Sb₂S₃) was prevented after HYDRODIS® GE inhibitor dosage. It

was observed that the structures seen in the filter were also cleaned, and the color formed on the filter turned into very weak orange. The fact that no scale formation was observed in Filter B, which was opened for control purposes and regularly monitored during the trial period, showed that the surface inhibitor we used works properly.

Table 1. The effect of HYDRODIS® GE products on scales of filters. i. The filter checked before trial, ii. The filter checked in the first week during the trial iii. The filter checked the second week during trial.

Date	Filter Location	Filter Images	Scales Images	Xrf Results																																																								
i. 25.11.2020	Jes-2 Rejection B Filter			<table border="1"> <thead> <tr> <th>Name</th> <th colspan="2">Class</th> <th>Date</th> <th>Time</th> <th>Duration</th> </tr> </thead> <tbody> <tr> <td>TRK JES 2 ÇIKIS REENJ. B FİLTRESİ</td> <td>Mining</td> <td>LE-FP</td> <td>25/11/2020</td> <td>16:43:13</td> <td>60 s</td> </tr> <tr> <td>Element</td> <td>Sb %</td> <td>S %</td> <td>Si %</td> <td>Fe %</td> <td>Ca %</td> <td>Pd %</td> <td>Ba %</td> <td>Mg %</td> <td>K %</td> <td>Sr %</td> </tr> <tr> <td>±</td> <td>0.000</td> </tr> <tr> <td>Element</td> <td>Mn %</td> <td>Cr %</td> <td>As %</td> <td>Sn %</td> <td>Co %</td> <td>Ag %</td> <td>Cd %</td> <td>Au %</td> <td>Ni %</td> <td>Hg %</td> </tr> <tr> <td>±</td> <td>0.42</td> <td>0.36</td> <td>0.15</td> <td>0.14</td> <td>0.07</td> <td>0.06</td> <td>0.06</td> <td>0.04</td> <td>0.04</td> <td>0.03</td> </tr> </tbody> </table>	Name	Class		Date	Time	Duration	TRK JES 2 ÇIKIS REENJ. B FİLTRESİ	Mining	LE-FP	25/11/2020	16:43:13	60 s	Element	Sb %	S %	Si %	Fe %	Ca %	Pd %	Ba %	Mg %	K %	Sr %	±	0.000	0.000	0.000	0.000	0.000	0.000	0.000	0.000	0.000	0.000	Element	Mn %	Cr %	As %	Sn %	Co %	Ag %	Cd %	Au %	Ni %	Hg %	±	0.42	0.36	0.15	0.14	0.07	0.06	0.06	0.04	0.04	0.03
Name	Class		Date	Time	Duration																																																							
TRK JES 2 ÇIKIS REENJ. B FİLTRESİ	Mining	LE-FP	25/11/2020	16:43:13	60 s																																																							
Element	Sb %	S %	Si %	Fe %	Ca %	Pd %	Ba %	Mg %	K %	Sr %																																																		
±	0.000	0.000	0.000	0.000	0.000	0.000	0.000	0.000	0.000	0.000																																																		
Element	Mn %	Cr %	As %	Sn %	Co %	Ag %	Cd %	Au %	Ni %	Hg %																																																		
±	0.42	0.36	0.15	0.14	0.07	0.06	0.06	0.04	0.04	0.03																																																		
ii. 3.12.2020	Jes-2 Rejection B Filter			<table border="1"> <thead> <tr> <th>Name</th> <th colspan="2">Class</th> <th>Date</th> <th>Time</th> <th>Duration</th> </tr> </thead> <tbody> <tr> <td>TRK - JES 2 ÇIKIS B FİLTRESİ</td> <td>Mining</td> <td>LE-FP</td> <td>03/12/2020</td> <td>11:03:48</td> <td>60 s</td> </tr> <tr> <td>Element</td> <td>Si %</td> <td>Sb %</td> <td>Mg %</td> <td>S %</td> <td>Ca %</td> <td>Fe %</td> <td>Pd %</td> <td>Ba %</td> <td>K %</td> <td>P %</td> </tr> <tr> <td>±</td> <td>19.60</td> <td>19.01</td> <td>5.73</td> <td>5.63</td> <td>5.06</td> <td>2.77</td> <td>1.27</td> <td>0.84</td> <td>0.72</td> <td>0.46</td> </tr> <tr> <td>Element</td> <td>Mn %</td> <td>Sr %</td> <td>Al %</td> <td>Cr %</td> <td>As %</td> <td>Sn %</td> <td>Hg %</td> <td>Au %</td> <td>Ag %</td> <td>Co %</td> </tr> <tr> <td>±</td> <td>0.30</td> <td>0.27</td> <td>0.26</td> <td>0.19</td> <td>0.10</td> <td>0.05</td> <td>0.03</td> <td>0.02</td> <td>0.02</td> <td>0.01</td> </tr> </tbody> </table>	Name	Class		Date	Time	Duration	TRK - JES 2 ÇIKIS B FİLTRESİ	Mining	LE-FP	03/12/2020	11:03:48	60 s	Element	Si %	Sb %	Mg %	S %	Ca %	Fe %	Pd %	Ba %	K %	P %	±	19.60	19.01	5.73	5.63	5.06	2.77	1.27	0.84	0.72	0.46	Element	Mn %	Sr %	Al %	Cr %	As %	Sn %	Hg %	Au %	Ag %	Co %	±	0.30	0.27	0.26	0.19	0.10	0.05	0.03	0.02	0.02	0.01
Name	Class		Date	Time	Duration																																																							
TRK - JES 2 ÇIKIS B FİLTRESİ	Mining	LE-FP	03/12/2020	11:03:48	60 s																																																							
Element	Si %	Sb %	Mg %	S %	Ca %	Fe %	Pd %	Ba %	K %	P %																																																		
±	19.60	19.01	5.73	5.63	5.06	2.77	1.27	0.84	0.72	0.46																																																		
Element	Mn %	Sr %	Al %	Cr %	As %	Sn %	Hg %	Au %	Ag %	Co %																																																		
±	0.30	0.27	0.26	0.19	0.10	0.05	0.03	0.02	0.02	0.01																																																		
iii. 11.12.2020	Jes-2 Rejection B Filter			<table border="1"> <thead> <tr> <th>Name</th> <th colspan="2">Class</th> <th>Date</th> <th>Time</th> <th>Duration</th> </tr> </thead> <tbody> <tr> <td>TRK-RE ENJ. B POMPASI FİLTRESİ</td> <td>Mining</td> <td>LE-FP</td> <td>11/12/2020</td> <td>18:08:58</td> <td>60 s</td> </tr> <tr> <td>Element</td> <td>Si %</td> <td>S %</td> <td>Ca %</td> <td>Fe %</td> <td>Sb %</td> <td>Mg %</td> <td>Pd %</td> <td>Ba %</td> <td>K %</td> <td>Mn %</td> </tr> <tr> <td>±</td> <td>14.72</td> <td>14.72</td> <td>12.69</td> <td>6.44</td> <td>4.60</td> <td>2.98</td> <td>2.55</td> <td>1.84</td> <td>1.54</td> <td>0.81</td> </tr> <tr> <td>Element</td> <td>Sr %</td> <td>P %</td> <td>Sn %</td> <td>Cr %</td> <td>As %</td> <td>Co %</td> <td>Cd %</td> <td>Ag %</td> <td>Au %</td> <td>Ni %</td> </tr> <tr> <td>±</td> <td>0.075</td> <td>0.042</td> <td>0.029</td> <td>0.070</td> <td>0.030</td> <td>0.953</td> <td>0.014</td> <td>0.093</td> <td>0.016</td> <td>0.041</td> </tr> </tbody> </table>	Name	Class		Date	Time	Duration	TRK-RE ENJ. B POMPASI FİLTRESİ	Mining	LE-FP	11/12/2020	18:08:58	60 s	Element	Si %	S %	Ca %	Fe %	Sb %	Mg %	Pd %	Ba %	K %	Mn %	±	14.72	14.72	12.69	6.44	4.60	2.98	2.55	1.84	1.54	0.81	Element	Sr %	P %	Sn %	Cr %	As %	Co %	Cd %	Ag %	Au %	Ni %	±	0.075	0.042	0.029	0.070	0.030	0.953	0.014	0.093	0.016	0.041
Name	Class		Date	Time	Duration																																																							
TRK-RE ENJ. B POMPASI FİLTRESİ	Mining	LE-FP	11/12/2020	18:08:58	60 s																																																							
Element	Si %	S %	Ca %	Fe %	Sb %	Mg %	Pd %	Ba %	K %	Mn %																																																		
±	14.72	14.72	12.69	6.44	4.60	2.98	2.55	1.84	1.54	0.81																																																		
Element	Sr %	P %	Sn %	Cr %	As %	Co %	Cd %	Ag %	Au %	Ni %																																																		
±	0.075	0.042	0.029	0.070	0.030	0.953	0.014	0.093	0.016	0.041																																																		

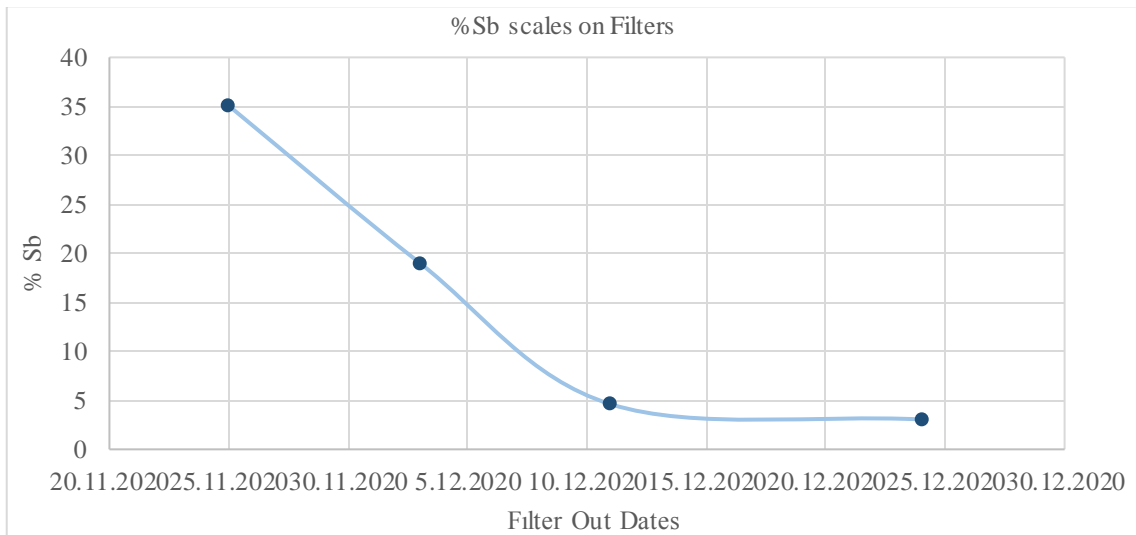


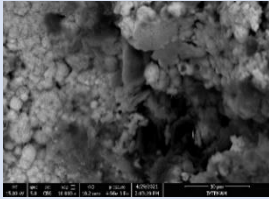
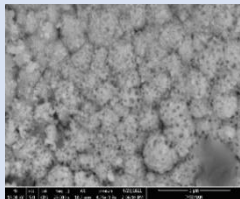
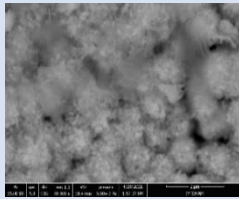
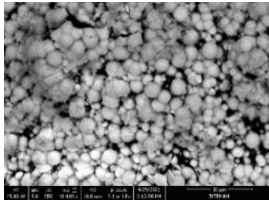
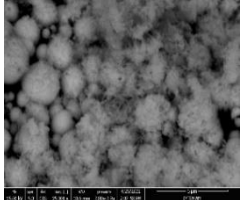
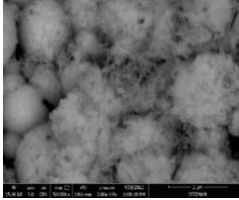
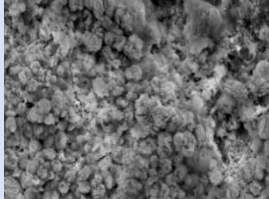
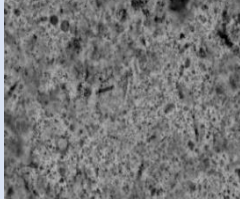
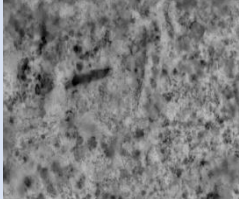
Figure 6. The effect of HYDRODIS® GE products on scales of filters.

3.3. The effect of HYDRODIS® GE on the scales of structures investigation with sem

In the scale samples examined by scanning electron microscopy (SEM), it was observed that the scale samples were knitted with a very tight needle network before the experiment was carried out, and the antimony combined with the free sulfur in the brine medium to form Stibnite compounds frequently and densely. After the HYDRODIS GE product was dosed, it was

observed that needle-like structures lost their pattern frequency and antimony produced less compounds with sulfur and the amount of Stibnite decreased. The obtained SEM images were supported by energy-dispersive x-ray spectroscopy (EDx) results taken from the regions where the images were. The effect of HYDRODIS® GE products on scales of structures investigation with SEM and EDx are given in Table 2 and Figure 7.

Table 2. The effect of HYDRODIS® GE products on the scales of structures investigation with sem. i. The scales of filters analyzed with sem and edx before trial, ii. The scales of filters analyzed with sem and edx in the first week during the trial iii. The scales of filters analyzed with sem and edx in the second week during trial.

Date	5-10 Micron Images	2-5 Micron Images	EDx Analyses	Elemental Ratio%																					
i. 25.11.2020				<table border="1"> <thead> <tr> <th>Element</th> <th>Wt%</th> <th>Atomic %</th> </tr> </thead> <tbody> <tr> <td>Mg</td> <td>0.20</td> <td>0.58</td> </tr> <tr> <td>Si</td> <td>0.28</td> <td>0.72</td> </tr> <tr> <td>S</td> <td>25.04</td> <td>55.41</td> </tr> <tr> <td>Sb</td> <td>70.35</td> <td>41.00</td> </tr> <tr> <td>Te</td> <td>4.12</td> <td>2.29</td> </tr> <tr> <td>Total:</td> <td>100.00</td> <td>100.00</td> </tr> </tbody> </table>	Element	Wt%	Atomic %	Mg	0.20	0.58	Si	0.28	0.72	S	25.04	55.41	Sb	70.35	41.00	Te	4.12	2.29	Total:	100.00	100.00
Element	Wt%	Atomic %																							
Mg	0.20	0.58																							
Si	0.28	0.72																							
S	25.04	55.41																							
Sb	70.35	41.00																							
Te	4.12	2.29																							
Total:	100.00	100.00																							
ii. 03.12.2020				<table border="1"> <thead> <tr> <th>Element</th> <th>Wt%</th> <th>Atomic %</th> </tr> </thead> <tbody> <tr> <td>Mg</td> <td>1.27</td> <td>3.49</td> </tr> <tr> <td>Si</td> <td>2.31</td> <td>5.48</td> </tr> <tr> <td>S</td> <td>25.53</td> <td>53.11</td> </tr> <tr> <td>Sb</td> <td>56.22</td> <td>30.80</td> </tr> <tr> <td>Ba</td> <td>14.66</td> <td>7.12</td> </tr> <tr> <td>Total:</td> <td>100.00</td> <td>100.00</td> </tr> </tbody> </table>	Element	Wt%	Atomic %	Mg	1.27	3.49	Si	2.31	5.48	S	25.53	53.11	Sb	56.22	30.80	Ba	14.66	7.12	Total:	100.00	100.00
Element	Wt%	Atomic %																							
Mg	1.27	3.49																							
Si	2.31	5.48																							
S	25.53	53.11																							
Sb	56.22	30.80																							
Ba	14.66	7.12																							
Total:	100.00	100.00																							
iii. 11.12.2020				<table border="1"> <thead> <tr> <th>Element</th> <th>Wt%</th> <th>Atomic %</th> </tr> </thead> <tbody> <tr> <td>Mg</td> <td>6.95</td> <td>12.32</td> </tr> <tr> <td>Si</td> <td>6.99</td> <td>10.73</td> </tr> <tr> <td>S</td> <td>46.96</td> <td>63.11</td> </tr> <tr> <td>Sb</td> <td>39.10</td> <td>13.84</td> </tr> <tr> <td>Total:</td> <td>100.00</td> <td>100.00</td> </tr> </tbody> </table>	Element	Wt%	Atomic %	Mg	6.95	12.32	Si	6.99	10.73	S	46.96	63.11	Sb	39.10	13.84	Total:	100.00	100.00			
Element	Wt%	Atomic %																							
Mg	6.95	12.32																							
Si	6.99	10.73																							
S	46.96	63.11																							
Sb	39.10	13.84																							
Total:	100.00	100.00																							

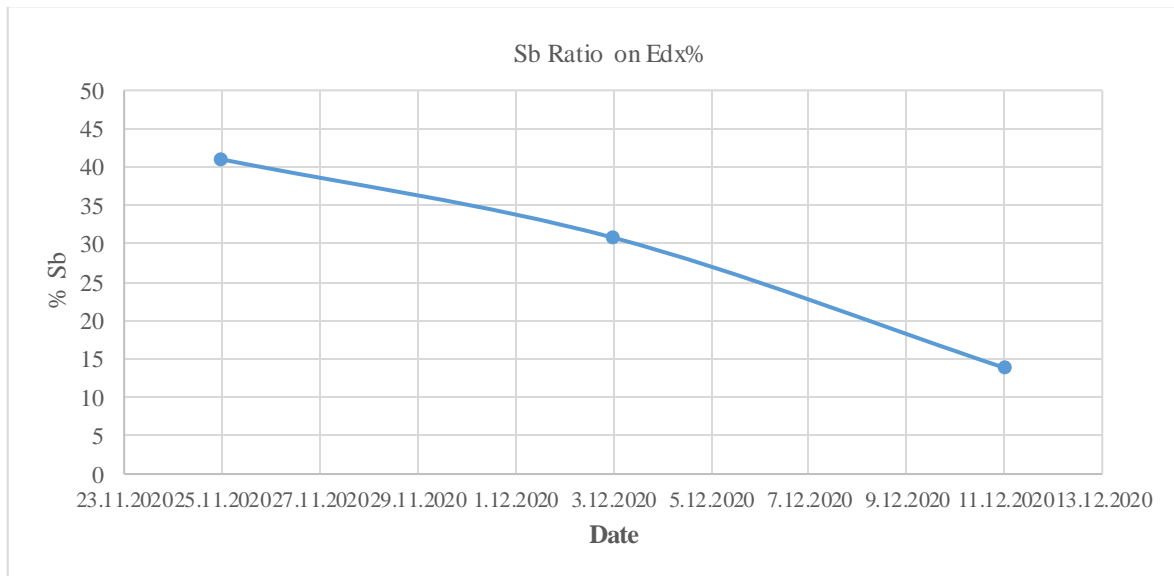


Figure 7. Scales of the structures at the reinjection filters % sb ratio on edx results.

3.4. Effect of HYDRODIS® GE on the scales of structures investigation with ft-ir

The peaks in my transmittance spectrum indicate that the compounds were changed with dosage. This is to be expected, and even is the desired outcome, because there was no hydrocarbon peak around 3000 cm⁻¹ during the second period of trial, indicating that there are no hydrocarbons present

on the scales samples. This is also shown in the spectra comparing the pre and post samples of stibnite against the background of air. Though the peaks are very similar, the lack of a hydrocarbon peak shows that the trial was successful. The two peaks are compared of this band are shifted 10 to 15 cm⁻¹ to a lower frequency, indicating that the receiver has switched to a stronger Sb⁺³ molecule collector for S. The visible spectrum can be assigned at ~1050 cm⁻¹, indicating that another strong band ν(C=S) has formed temporarily.

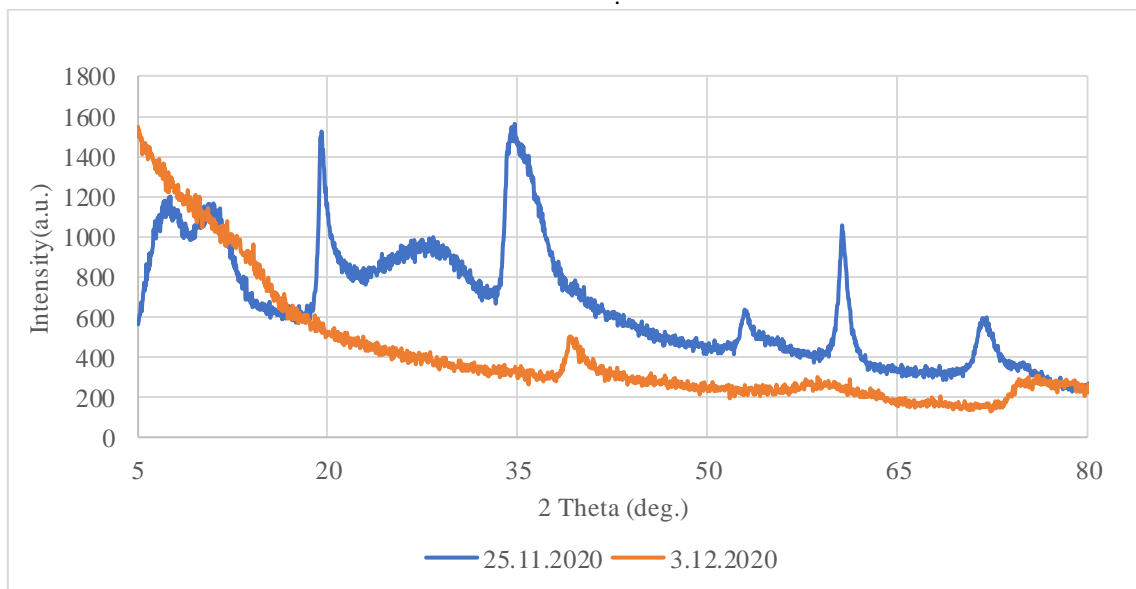


Figure 8. Xrd pattern of scales of the structures at the reinjection filters

4. DISCUSSION AND CONCLUSIONS

In this study, we claimed to prevent the stibnite issue. In the case of the study, we dosed different quantities of scale agents at the plant inlet. We gained different results and these results confirmed our hypothesis. These hypothesis confirmed by reducing the amount of precipitation on the coupons within the trial time. The reduction of the

temperature of the brine during the heat exchanging process, the stibnite scales prevented on the filters and pre-heaters even at 65 °C. The HYDRODIS GE® technology remarkably reduced the amount of precipitation of stibnite as observed on geothermal power plant's outlet coupons. The coupon images are given in Table 3.

The scales were analyzed by XRD, FT-IR, and other techniques. According to Table 3, the scale characterization data obtained during the study showed that the stibnite scales at lower outlet temperatures of geothermal power plants have been kept under control by decreasing the speed of the crystal growing using HYDRODIS GE® polymers. The minimum dosages have been checked during the trial period of the system and it could operate smoothly even at 5 ppm. The obtained results have shown that stibnite compounds can be blocked by using HYDRODIS polymer just at the entrance of the heat exchanger of the geothermal power plant. In addition to, the fact that the products at low dosage intervals stabilizes the power plant in a short time like one month during the prevention of the stibnite problem and its from the power plant, confirms the purpose and success of this study. All in all, in Table 3. added to the conclusion section covers a period of not only one month

but deals with the before and after of the problem. The visuals in Table 3 confirm that the reduced to growing-up crystalline structure and precipitation on the coupons have been prevented over time and that the HYDRODIS® GE products have successfully protected the system. According to the results obtained, this study showed that HYDRODIS® GE products can be applied in different power plants and preheaters designed for different temperatures under different dosage conditions.

Considering the scalable application of power plants and the aim of sustainable and stable brine chemistry, we expect that our work can be beneficial to the study of antimony compounds and provide a significant strategy for geothermal power plants.

Table 3. The evaluation coupons at the geothermal power plan

<i>Date</i>	<i>Coupon Location</i>	<i>Coupon Images</i>
<i>8.11.2019</i>	<i>Plant Outlet</i>	
<i>25.11.2020</i>	<i>Plant Outlet</i>	
<i>03.12.2020</i>	<i>Plant Outlet</i>	
<i>11.12.2020</i>	<i>Plant Outlet</i>	
<i>31.01.2021</i>	<i>Plant Outlet</i>	

Acknowledgements

We would like to thank all reservoir team of our partner for their support in this study.

REFERENCES

- Anderson, C. G. (2012). The metallurgy of antimony. Supplement 4. *Chemie der Erde*, 72(SUPPL.4), 3–8. <https://doi.org/10.1016/j.chemer.2012.04.001>
- Baran, K., Aksoy, N., Serpen, U., & Şişman, M. (2015). Stibnite Scaling in a Binary Power Plant in Turkey. *World Geothermal Congress 2015, April*, 19–25.
- Brown, K. (2011). *Antimony and Arsenic Sulfide Scaling in Geothermal Binary Plants*. May, 25–27.
- Haklıdır, F. S. T., & Şengün, R. (2020). Hydrogeochemical similarities and differences between high temperature geothermal systems with similar geologic settings in the Büyük Menderes and Gediz Grabens of Turkey. *Geothermics*, 83(August 2019). <https://doi.org/10.1016/j.geothermics.2019.101717>
- Krupp, R. E. (1988). Solubility of stibnite in hydrogen sulfide solutions, speciation, and equilibrium constants, from 25 to 350°C. *Geochimica et Cosmochimica Acta*, 52(12), 3005–3015. [https://doi.org/10.1016/0016-7037\(88\)90164-0](https://doi.org/10.1016/0016-7037(88)90164-0)
- Olsen, N. J., Mountain, B. W., & Seward, T. M. (2012). Experimental study of stibnite solubility in aqueous sulfide solutions from 25 to 90°C. *New Zealand Geothermal Workshop*, 19(November).
- Scanes, C. G. (1989). Notice concerning copyright restrictions. *Growth, Development, and Aging*, 53.
- Sherman, D. M., Ragnarsdottir, K. V., & Oelkers, E. H. (2000). Antimony transport in hydrothermal solutions: An EXAFS study of antimony(V) complexation in alkaline sulfide and sulfide-chloride brines at temperatures from 25°C to 300°C at P(sat). *Chemical Geology*, 167(1–2), 161–167. [https://doi.org/10.1016/S0009-2541\(99\)00207-7](https://doi.org/10.1016/S0009-2541(99)00207-7)
- Weres, O. (2019). Chemistry of stibnite, orpiment and other sulfide minerals deposited from geothermal brines. *Transactions - Geothermal Resources Council*, 43, 690–703.